Gene Expression and Alzheimer's Disease

Evaluation of Gene Expression Patterns in Brain and Blood for an Alzheimer's Disease

Mouse Model

Amanda Házy

A Senior Thesis submitted in partial fulfillment
of the requirements for graduation
in the Honors Program
Liberty University
Spring 2015

Acceptance of Senior Honors Thesis

This Senior Honors Thesis is accepted in partial
fulfillment of the requirements for graduation from the
Honors Program of Liberty University.

_____
Gary D. Isaacs, Ph.D.
Thesis Chair

_____
Kimberly Mitchell, Ph.D.
Committee Member

_____
Russell Yocum, Ed.D.
Committee Member

_____
Brenda Ayres, Ph.D.
Honors Director

_____
Date

Abstract

Previous studies have established a causative role for altered gene expression in development of Alzheimer's disease (AD). These changes can be affected by methylation and miRNA regulation. In this study, expression of miRNA known to change methylation status in AD was assessed by qPCR. Genome-wide expression changes were determined by RNA-sequencing of mRNA from hippocampus and blood of control and AD mice. The qPCR data showed significantly increased expression of Mir 17 in AD, and sequencing data revealed 230 genes in hippocampus, 58 genes in blood, and 8 overlapping genes showing significant differential expression (p value ≤ 0.05). Expression data from this study revealed novel gene expression changes affecting AD and identified changing genes in blood as potential AD biomarkers.

Gene Expression and Alzheimer's Disease: Evaluation of Gene Expression Patterns

in Brain and Blood in an Alzheimer's Disease Mouse Model

Alzheimer's disease (AD) is a neurodegenerative disorder characterized by accumulation of amyloid beta (AB) plaques in the brain and loss of neuronal cells with a corresponding decrease in cognitive function [1]. As one of the foremost health challenges in developed countries, AD affects large numbers of people in a variety of environments [2]. Understanding the biological events involved in AD pathology and determining accurate means of early detection are crucial areas of research. While many researchers have investigated the development of AB plaques and other characteristics of the disease, little is known about the initial causes of AD and the specific biochemical processes of AD development. Analysis of changes in gene expression associated with AD pathology is one important area of current AD research. The development of AD is largely directed by increases and decreases in activity of specific genes related to the disease, and understanding these changes will give better understanding of the process of disease as well as insights into possible treatments. Obtaining a profile of genes that affect AD progression could also be used to develop a diagnostic test for this disease. In pursuance of these goals, my research evaluated changes in gene expression in brain and blood using a mouse model of Alzheimer's disease.

AD and Gene Expression

Alzheimer's Disease

Alzheimer's disease is a progressive neurodegenerative disorder that causes a slow but irreversible loss of cognitive ability. The disease is marked by distinctive neuronal amyloid-beta plaques derived from amyloid precursor protein (APP) as well as

by neurofibrillary tangles (NFTs) formed by hyperphosphorylated tau protein [3, 4]. These protein deposits are often accompanied by neuroinflammation and result in eventual neuronal cell death. Many regions of the brain are affected as AB plaques and NFTs form, most notably the hippocampus and neocortex. As the disease develops and neurons die, the patient exhibits the cognitive dysfunction and behavioral changes diagnostic of clinical dementia. Initial memory loss progresses to speech difficulty and problems with the performance of everyday tasks such as driving or making phone calls [4, 5]. This disease affects approximately 15 million people worldwide, and there is no known cure. Diagnosis of the disease is challenging as well, since many of the symptoms of AD (memory loss, difficulty with daily activities, behavioral changes) resemble the signs of normal aging [4]. An autopsy with a histopathological examination of the brain to identify AB plaques and NFTs is required for definitive clinical diagnosis of the disease [5]. In addition, causes of the disease are largely unknown. Mutations in the APP (amyloid precursor protein) and PSEN1 (presenilin 1) genes have been shown to cause AD by increasing deposition of AB plaques, but most AD cases cannot be traced back to a specific genetic mutation [5, 6]. With the large number of people affected by AD, determination of the causes, diagnosis, and treatment of the disease is an active area of current research.

Effects of Gene Expression in AD

Changes in gene expression are known to influence the progression of AD in the brain. Like other neurodegenerative diseases, AD involves complex interactions between many different factors in the brain over an extended time period. The disease develops when specific genes alter their expression patterns (i.e. increase or decrease transcription

of the genes to form mRNA, with a corresponding increase or decrease in the protein

products of these genes). For example, in order for AB to deposit as senile plaques on the

brain, APP must be processed by secretase enzymes to form toxic AB peptides. This

requires an increase in expression of the APP gene to form high amounts of the precursor

protein as well as changes in expression of secretase enzymes to form AB plaques [7, 8].

Many other genes have also been implicated in AD including those involved in stress

response, inflammation, apoptosis, angiogenesis, and transcriptional regulation [9]. As

these changes lead to deposition of AB, the AB plaques themselves further influence

gene expression to continue disease development. Toxic AB plaques are known to cause

changes in expression of transcription factors, cell-cycle related genes, and genes

involved in growth factor regulation in the hippocampus and cortex [10, 11]. Current

research focuses on the continuing investigation of genes known to be involved with AD

as well as the discovery of relevant genes not yet linked to the disease. The overall goal is

to fully understand this disease to determine effective methods of diagnosis and

treatment.

Epigenetic Control of Gene Expression

Gene expression can be controlled by epigenetic modifications (chemical

modifications to genes that do not alter the DNA base sequence), and many studies have

demonstrated a connection between AD and these epigenetic changes [6, 12, 13].

Previous research has specifically investigated the role of DNA methylation in gene

expression and AD development [14-18]. DNA methylation involves the addition of a

methyl group to a cytosine base, forming methylated cytosine (5-mC). Methylation

decreases gene expression by repressing transcription of the methylated gene. According

to studies of the connection between methylation and AD, accumulation of AB and

progression of AD pathology involve both increases in methylation (hypermethylation)

and decreases in methylation (hypomethylation) in different areas of the genome [19].

Methylation-dependent gene silencing has been directly linked to AD pathology, and

several of the specific genes affected have been identified [20]. Since alterations in

methylation status and corresponding changes in gene expression are known to affect

AD, current research continues to investigate these changes.

Gene expression in AD can also be influenced by post-transcriptional regulation

via noncoding gene transcripts called microRNA (miRNA). MicroRNAs are small, ~22

nucleotide-long sequences of RNA that are complementary to sections of the 3'

untranslated region (UTR) of mRNA targets [21]. Genes coding for miRNA can be

located in introns, exons, or intergenic regions. These genes are transcribed to form long

primary miRNAs which are then processed by enzymes including the Drosha complex

and Dicer to form the final miRNA. This miRNA joins Argonaute proteins to form the

RNA-induced silencing complex (RISC), which functions in translational repression.

When miRNA pairs to complementary mRNA targets, the miRNA can either inhibit

translation of the gene product or lead to degradation of the mRNA [22]. Post-

transcriptional regulation through miRNA is known to play a role in the development of

many diseases including AD [22, 23]. In addition, miRNA expression is itself frequently

regulated by methylation [21]. Analysis of AD-related changes in miRNA and

methylation with the corresponding changes in gene expression is needed for full

understanding of the disease.

Altered Gene Expression Patterns in Other Tissues

While neuronal tissue displays the most distinctive changes in gene expression with AD, other tissues have also been shown to have altered expression in certain genes. These specific expression changes show promise as potential biomarkers for diagnosis of the disease. Definitive AD diagnosis currently requires an autopsy to examine the brain for AB plaques and NFTs [5]. Since clinical diagnosis relies on behavioral signs and can be difficult early in disease progression, tissues other than brain have been investigated in search of diagnostic biomarkers. Some researchers have tested cerebrospinal fluid (CSF) to determine whether levels of mRNA and protein change consistently during AD progression and could be used to diagnose or predict disease development. Promising targets for CSF biomarkers include AB and tau peptides, insulin-like growth factor binding proteins, and various other genes and proteins linked to the disease [10, 24]. AD biomarkers in blood have also been investigated with the goal of developing a simple blood test for AD diagnosis. Gene expression changes in characteristic ways in the blood during AD development, and some of these alterations parallel changes seen in the brain [25]. Ongoing studies focus on identifying the specific changes in blood gene expression in AD, understanding their role in disease development and correlation with brain expression changes, and determining a blood gene expression profile useful for early AD diagnosis.

<center>**Experimental Design**</center>

To investigate gene expression, this research utilized a transgenic mouse model of AD. Transgenic animal models have been useful in the study of many disease states due to their ability to mimic human disease development, and several mouse models have

been used in previous AD research. One of the earliest mouse models for AD involved

mice carrying the human APP gene. Mice carrying this transgene expressed human APP

and were used to examine the development of amyloid plaques in AD [7]. For this

research, the 5XFAD mouse model carrying five mutations associated with familial

Alzheimer's disease (FAD) was used. This mouse model is commercially available and

was created by transgene injection into C57/B6XSJL hybrid pronuclei. These mice carry

the APP and PSEN1 transgenes under control of the mouse Thy1 promoter. Three

mutations in the APP gene and two mutations in the PSEN1 gene lead to high expression

of both amyloid precursor protein and presenilin 1, with corresponding development of

AB plaques. In these mice, neuronal amyloid-beta plaques begin to develop at two

months of age. Neurodegeneration and loss of memory proceed in these mice in a parallel

pathway to AD development in humans, making them ideal for AD research [26].

This research analyzed changes in gene expression in brain and blood using the

5XFAD mouse model of Alzheimer's disease. Changes in expression of specific miRNA

known to change methylation status in hippocampus were analyzed using the miScript

PCR procedure from Qiagen to assess the interactions between methylation, miRNA

regulation, and gene expression in AD. Genome-wide expression patterns in

hippocampus were also assessed to determine which genes change in AD and how these

changes affect disease development. The hippocampus was chosen for this analysis due

to known effects of AD on the hippocampus throughout disease development as well as

the established correlation between AB in the hippocampus and the severity of AD

progression [27, 28]. In addition, a gene expression profile for blood samples was

investigated to determine how the blood is affected in AD. Data from blood samples and

hippocampus collected from 5XFAD mice were compared to evaluate which gene changes were consistent in both samples and could be targeted as AD biomarkers. To determine differential gene expression, total RNA was isolated from hippocampus and blood of both AD and control mice (three male AD mice and three female control mice). The mRNA was then purified, converted to cDNA, and sequenced using an Illumina MiSeq gene sequencer (Supp. Figure 1). This process gave data detailing the base sequences and relative abundances of all gene transcripts contained in the samples. RNA-Seq analysis was performed using the Tuxedo suite for RNA-Seq analysis including BowTie, TopHat, Cufflinks, Cuffdiff, and CummeRbund (Supp. Figure 2). The resulting data were evaluated to determine which genes displayed altered expression in the AD brain and which genes in blood could be useful as biomarkers for AD.

Methods

RNA Isolation

Total RNA was isolated from hippocampus and blood of three transgenic male AD mice and three normal female control mice aged 10-12 months. Mice were anesthetized with dry ice and sacrificed by decapitation. Hippocampi were dissected out, and blood was collected by cardiac puncture. To isolate hippocampal RNA, hippocampi were homogenized in 1 mL Trizol/50-100 mg tissue (Invitrogen). Blood samples were placed in EDTA tubes and centrifuged for 10 min. to isolate cells before 100 uL cells/sample were homogenized in 1 mL Trizol. After incubation at room temperature for 5 min., 0.2 mL chloroform were added per 1 mL Trizol. Samples were centrifuged at 12,000 x g for 15 min. and the aqueous phase was removed to extract RNA. To precipitate the RNA, 0.5 mL isopropanol were added per 1 mL Trizol, incubated for 10

min. at 4 ℃, and centrifuged at 12,000 x g for 10 min. RNA pellets were washed with

75% ethanol, centrifuged at 12,000 x g for 5 min., air-dried, and resuspended in 50 uL

RNAse free water.

Analysis of miRNA Expression

Differential expression of four miRNA genes was evaluated using the miScript

PCR system (Qiagen). miRNA genes of interest were identified based on previously

determined changes in methylation status of these genes. Earlier work using chromatin

immunoprecipitation and microarray identified Mir 17, Mir 26b, and Mir 92 as

hypomethylated in AD, while Mir 702 was identified as hypermethylated in AD. To

determine changes in miRNA expression, miRNA was reverse transcribed to cDNA

using miScript reverse transcriptase. The miScript reverse transcription reaction

contained both a reverse transcriptase and a poly(A) polymerase to both adenylate

miRNA and allow its conversion to cDNA. The oligo-dT primers used in this reaction

contained a universal tag sequence on the 5' end which allowed specific amplification of

miRNA in subsequent reactions. Each reverse transcription reaction contained 500 ng

total RNA, 4 uL 5X miScript HiFlex Buffer, 2 uL 10X miScript Nucleics Mix, 2 uL

miScript Reverse Transcriptase Mix, and RNase-free water to a total volume of 20 uL.

Each reaction was incubated for 30 min. at 37 ℃ before the enzyme was inactivated by

incubation for 5 min. at 95 ℃. Samples were then diluted to a final cDNA concentration

of 2.5 ng/uL for qPCR analysis of gene expression for specific miRNA.

Differential expression of specific miRNA was determined by qPCR using

miScript Universal Primer (complementary to the tag sequence added in reverse

transcription) as the reverse primer for qPCR reactions and miScript Primer Assays

specific to the miRNA of interest as the forward primer for each reaction (Qiagen). Each

qPCR reaction contained 12.5 uL 2X Quantitect SYBR Green PCR Master Mix, 2.5 uL

10X miScript Universal Primer, 2.5 uL 10X miScript Primer Assay, 2 uL template

cDNA, and 5.5 uL water. For each gene of interest, a serial dilution of control cDNA

samples (1, 1:10, and 1:100) and a 1:10 dilution of AD cDNA were tested. Samples were

amplified using the following PCR scheme: 95 ℃ for 15 min.; 40 cycles of 94 ℃ for 15

sec, 55 ℃ for 30 sec, 70 ℃ for 30 sec. Fold change was calculated with reference to

control genes (Gapdh and Tubb3). Cq values from control cDNA samples were used to

construct a standard curve for calculation of initial fold, and this value was divided by

average fold of the two control genes to determine fold change.

mRNA Purification

mRNA was isolated from total RNA using a TruSeq Stranded mRNA Sample

Preparation kit (Illumina). First, 2 ug total RNA from each sample were diluted in 50 uL

RNAse-free water and 50 uL RNA Purification Beads were added to bind polyadenylated

mRNA with the oligo-dT magnetic beads. After mixing, RNA was denatured and bound

to the beads by incubation at 65 ℃ for 5 min. and returned to 4 ℃, followed by

incubation at room temperature for 5 min. Samples were placed on a magnetic stand for 5

min. to remove the beads, and supernatant was discarded. Beads were washed with 200

uL Bead Washing Buffer, mixed, and beads were removed as before. Supernatant was

discarded and 50 uL Elution Buffer were added and mixed. RNA was then eluted by

incubation at 80 ℃ for 2 min. and brought to 25 ℃. In a second round of mRNA

purification, 50 uL Bead Binding Buffer were added to facilitate mRNA rebinding to the

beads, mixed, and incubated at room temperature for 5 min. Beads were removed,

supernatant was discarded, and beads were washed as before. Beads were then removed

from the Bead Washing Buffer, and supernatant was discarded.

cDNA Preparation

RNA was converted to double-stranded cDNA using MMLV reverse

transcriptase. For synthesis of the first cDNA strand, 19.5 uL Fragment, Prime, Finish

Mix containing random hexamers as reverse transcriptase primers were added to each

sample tube holding mRNA-bound magnetic beads and mixed. Samples were incubated

at 94 ℃ for 8 min. and returned to 4 ℃ to elute and prime the RNA for reverse

transcription. After samples were centrifuged, beads were removed as before, and 17 uL

supernatant containing the eluted RNA were transferred to new tubes. For the first-strand

cDNA synthesis reaction, 8 uL First Strand Synthesis Mix (10% MMLV reverse

transcriptase, 90% First Strand Synthesis Act D Mix) were added to each sample and

single-stranded cDNA was synthesized using the following PCR scheme: 25 ℃ for 10

min., 42 ℃ for 15 min., 70 ℃ for 15 min., hold at 4 ℃. Before second strand synthesis, 5

uL End Repair Control diluted 1:50 in Resuspension Buffer were added to each sample.

To synthesize the second cDNA strand, 20 uL Second Strand Marking Master Mix were

added and incubated at 16 ℃ for 1 hour before bringing the samples to room temperature.

This second incubation yielded double-stranded cDNA.

The cDNA was further purified using magnetic beads to prepare for sequencing.

To remove undesired RNA or contaminants from the cDNA samples, 90 uL AMPure XP

beads were added to each sample containing 50 uL cDNA and incubated at room

temperature for 15 min. Beads were removed as before and 135 uL supernatant was

discarded from each sample. The beads were then washed twice with 200 uL 80% EtOH

and allowed to air dry for 15 min. To resuspend the cDNA, 17.5 uL Resuspension Buffer were added and incubated at room temperature for 2 min. before beads were removed and 15 uL supernatant containing cDNA were transferred to new tubes.

Sequencing Preparation

The cDNA samples were adenylated and ligated to unique adapter sequences to allow hybridization with the sequencing flow cell and allow identification of separate samples during sequencing. To facilitate adenylation of the samples, 2.5 uL A-Tailing Control diluted 1:100 in Resuspension Buffer were added to each sample before 12.5 uL A-Tailing Mix were added and incubated at 37 ℃ for 30 min. This was followed by incubation at 70 ℃ for 5 min. before samples were returned to 4 ℃. After adenylation, 2.5 uL Ligation Control diluted 1:100 in Resuspension Buffer were added to each sample as well as 2.5 uL Ligation Mix. To allow differentiation of samples during sequencing, 2.5 uL of a unique RNA Adapter Index were added per sample and incubated at 30 ℃ for 10 min. before 5 uL Stop Ligation Buffer were added to end the ligation reaction.

Samples were further purified and amplified to prepare for sequencing. In the first purification step, 42 uL AMPure XP beads were added and incubated at room temperature for 15 min. Beads were removed as before and 79.5 uL supernatant were discarded before the beads were washed twice with 200 uL 80% EtOH. The samples were allowed to air-dry for 15 min. before 52.5 uL Resuspension Buffer were added and incubated at room temperature for 2 min. After 50 uL supernatant were collected, 50 uL AMPure XP beads were added and the purification process was repeated, discarding 95 uL supernatant and resuspending the beads in 22.5 uL Resuspension Buffer. Beads were removed and 20 uL supernatant were collected for PCR amplification. To create cDNA

pools for sequencing, 5 uL PCR Primer Cocktail and 25 uL PCR Master Mix were added

to each sample before amplification using the following PCR scheme: 98 ℃ for 30 sec;

15 cycles of 98 ℃ for 10 sec, 60 ℃ for 30 sec, 72 ℃ for 30 sec; 72 ℃ for 5 min., hold at

4 ℃. For a final round of purification, 50 uL AMPure XP beads were added and

incubated at room temperature for 15 min. Beads were removed and 95 uL supernatant

were discarded before washing the beads twice with 200 uL 80% EtOH. Samples were

allowed to air-dry at room temperature for 15 min. before 32.5 uL Resuspension Buffer

were added and incubated at room temperature for 2 min. Beads were then removed and

30 uL supernatant containing purified cDNA were collected for sequencing.

Quantification and Sequencing

Samples were quantified by qPCR prior to sequencing. Tenfold sample dilutions

were prepared up to 10^{-6}, and qPCR reactions were run in triplicate for each sample.

KAPA Library Quantification Standards ranging from 20 pM to 0.0002 pM (KAPA

Biosystems) were used to construct a standard curve. Each qPCR reaction contained 2.5

uL primer mix (primers designed to match Illumina adapter sequences ligated to the

samples during preparation), 12.5 uL SYBR Green Master Mix (Life Technologies), 5 uL

water, and 5 uL sample. Samples were amplified using the following PCR scheme: 95 ℃

for 5 min.; 35 cycles of 95 ℃ for 30 sec, 60 ℃ for 45 sec. Concentrations were calculated

in pM, and the average value from each triplicate series was used as the concentration of

each sample for loading into the sequencer.

Samples were denatured and diluted to 12 pM before loading into the Miseq

sequencer. Each sample was initially diluted to 4 nM, and separate samples were pooled

(3 samples per sequencing run). To denature the cDNA, 5 uL 0.2 N NaOH were added to

5 uL sample and incubated for 5 min. at room temperature. Following denaturation, 990

uL chilled Hybridization Buffer were added to give a 20 pM library in 1 mM NaOH. The

20 pM library was further diluted to 12 pM in Hybridization Buffer. A PhiX control

(Illumina) was also prepared to increase quality of the sequencing run. To prepare the

PhiX control, 10 nM PhiX library was diluted to 4 nM with 10 mM Tris-Cl, pH 8.5 with

0.1% Tween-20. The PhiX control was then denatured and diluted in the same way as the

cDNA samples before combining with the sample to be loaded (PhiX spike-in ranged

from 5%-20% in multiple sequencing runs). A 600 uL sample was then loaded into the

sequencing cartridge and sequenced using an Illumina MiSeq.

Data Analysis

Initial sequencing data was assessed by quality score and prepared for

downstream analysis using the Galaxy platform. During each sequencing run, the MiSeq

sequencer generated DNA base sequences in FastQ file format. Files contained quality

scores for each run in addition to the base sequence reads mapped to individual samples

by the unique adapter indexes ligated to each one. Initial run quality was evaluated by

QScore ≥ 30 and other quality assessments using the Illumina BaseSpace cloud

computing environment. FastQ files generated by each run were then uploaded to the

Galaxy server for differential expression analysis. The FastQ Groomer tool was used to

prepare the initial files for further analysis by confirming that the sequence data and

quality scores were in FastQ Sanger format, which is required for downstream RNA-Seq

analysis using the Tuxedo suite [29].

Sequencing data was analyzed for differential expression using the Tuxedo suite

for RNA-Seq analysis (via the Galaxy platform). First, FastQ files were aligned to the

mm9 reference genome using TopHat and BowTie. The TopHat for Illumina program on

the Galaxy server maps splice junctions between exons as the BowTie short read aligner

matches base sequences to the reference genome [30]. Since sequencing generated

paired-end reads for each sample (i.e. read each cDNA fragment once left to right and

once right to left), two separate FastQ files (Read 1 and Read 2) were run through the

TopHat/BowTie program using the mate-paired library setting for each sample.

Aligned sequencing reads were then analyzed using Cufflinks to assemble

expressed transcripts and determine FPKM values for each transcript (Fragments Per

Kilobase of transcripts per Million mapped reads, i.e. normalized transcript counts).

Accepted hits from TopHat were run through the Cufflinks program using maximum

intron length of 300,000, minimum isoform fraction 0.1, pre mRNA fraction 0.15,

quartile normalization (eliminating the top 25% of genes from the FPKM denominator),

bias correction, multi-read correct, and effective length correction. The RefFlat table for

the mm9 genome downloaded from UCSC was used as the reference annotation for

Cufflinks. This gave FPKM values for each expressed transcript in each sample mapped

to specific genes. The Cuffmerge program was used to create a list of acceptable

transcripts for differential expression analysis by merging all six Cufflinks files (n=3 for

control and AD mice) with RefFlat as the reference annotation. Cuffdiff was then used to

determine differential transcript expression, splicing, and promoter use [31]. Using

Cuffdiff, aligned sequencing reads (accepted hits) from TopHat for control samples were

compared to aligned reads for AD samples against the background of accepted transcripts

from Cuffmerge. The analysis used geometric normalization, a pooled dispersion

estimate method, an allowed false discovery rate of 0.05, minimum alignment count of

10, multi-read correct, bias correction, the mm9 genome, and read group datasets. The Cuffdiff and Cufflinks output files were then converted to csv format to allow analysis using Microsoft Excel. Finally, data were visualized using CummeRbund [32]. Gene ontology was assessed using the GeneCodis program [33-35].

Selection of Control Genes

Gapdh (glyceraldehyde-3-phosphate dehydrogenase) and Tubb3 (beta-tubulin 3) were selected as control genes for qPCR confirmation of differential gene expression. Five genes (Actb, Gapdh, Pagr1a, Ak1, and Tubb3) were initially tested as potential control genes. These genes were chosen based on empirical data collected from sequencing runs. Primers were designed for each potential control gene using Primer3 (http://biotools.umassmed.edu/bioapps/primer3_www.cgi). All genes were evaluated by qPCR to determine fold change between control and AD samples. Gapdh and Tubb3 were chosen as control genes based on five criteria. First, acceptable primers gave consistent melt curves with one peak, confirming amplification of one product. Second, qPCR of serial cDNA dilutions for acceptable control genes gave an $R^2 \geq 0.98$. Third, control genes gave consistent fold changes from control to AD over successive qPCR runs, indicating an accurate reflection of sample composition. Fourth, genes considered as controls showed little to no differential expression based on sequencing data. Finally, primer efficiencies for the chosen control genes were consistently near 1 (exponential doubling near 2). Based on these criteria, Gapdh and Tubb3 were selected as control genes for use in all sequencing confirmations using qPCR.

qPCR Confirmation of Gene Expression

cDNA pools for qPCR confirmations of differential expression were constructed for each sample using a miScript RT kit (Qiagen). For each reverse transcription reaction, 500 ng total RNA were combined with 4 uL 5x HiFlex Buffer, 2 uL 10x miScript Nucleics Mix, and 2 uL miScript Reverse Transcriptase Mix before bringing up to a final volume of 20 uL with RNAse-free water. This RT-PCR reaction was incubated at 37 ℃ for 60 min. before the reverse transcriptase was inactivated by incubation at 95 ℃ for 5 min. The resulting single-stranded cDNA was diluted to 2.5 ng/uL for use in qPCR confirmations of differential expression.

Gene-by-gene differential expression was confirmed using qPCR with the cDNA pools. After genes of interest were identified by sequencing, primers for each gene were designed using Primer3. Fold change from control to AD was then determined for n=3 samples by qPCR. Each qPCR reaction contained 12.5 uL 2x QuantiTect SYBR Green PCR Master Mix, 2.5 uL 10x primer mix, 2 uL cDNA, and 8 uL RNAse-free water. For each gene tested, a serial dilution of control cDNA samples (1, 1:10, and 1:100) and a 1:10 dilution of AD cDNA were tested. Samples were amplified using the following PCR scheme: 95 ℃ for 15 min.; 40 cycles of 94 ℃ for 15 sec, 55 ℃ for 30 sec, 70 ℃ for 30 sec. Fold changes were calculated as previously described.

Results

MicroRNA 17

Analysis of miRNA expression using the miScript qPCR system (Qiagen) found a significant increase in transcript abundance of microRNA 17 (Mir 17) in the AD hippocampus. Mir 17, Mir 26b, Mir 92, and Mir 702 were assessed for differential

expression based on known changes in methylation status shown by previous work with

methylation-specific chromatin immunoprecipitation and promoter microarray.

Microarray data indicated that Mir 17 was significantly hypomethylated in the AD

hippocampus compared to control hippocampus. This suggests that the Mir 17 gene

would show increased expression in AD, since methylation is typically associated with

gene repression. Expression analysis using qPCR confirmed significantly increased

expression of Mir 17 (1.66 fold increase) in AD (Figure 1). Mir 26b, Mir 92, and Mir 702

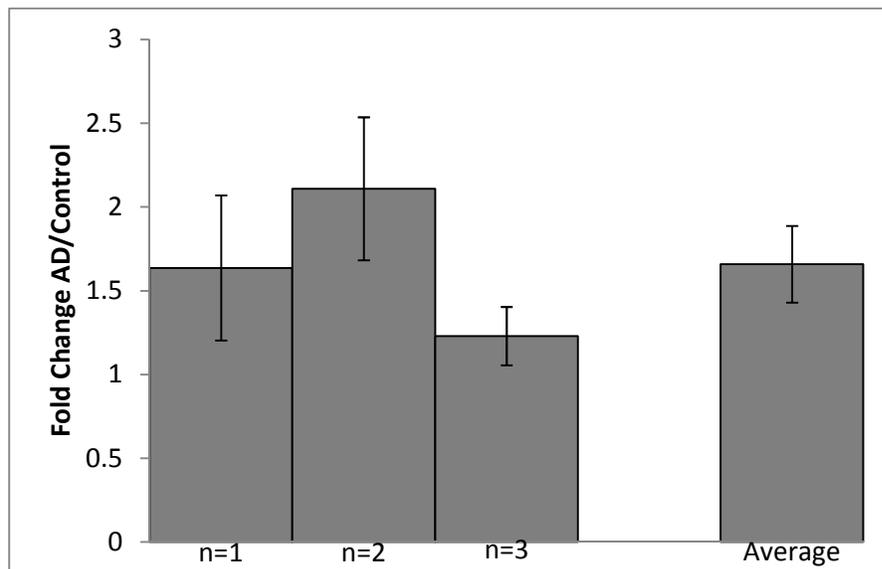showed no significant AD-related changes in expression.

Figure 1. Increased expression of Mir 17. Analysis using qPCR showed increased expression of Mir 17

in AD hippocampus (1.66 average fold increase). Mir 17 transcript abundances in hippocampus for three

AD and three control mice were compared using qPCR to determine fold change of Mir 17 in AD. Fold

change was calculated for each replicate using two control genes (Gapdh and Tubb3), and error bars show

SEM for each replicate based on the variance between control genes.

Genome-wide Differential Gene Expression in Mouse Hippocampus

Initial Cuffdiff analysis of RNA-sequencing data from three control and three AD

mice revealed 2250 genes showing altered expression in AD hippocampus (Figure 2).

Statistical significance was assessed using p values calculated by the Cuffdiff program.

This analysis found 230 genes with significant changes in expression in AD hippocampus

(p value ≤ 0.05), with 22 genes showing a p value ≤ 0.0005 (Supp. Table 1 and 2). This

gene list included many genes with known connections to AD and neurobiology in

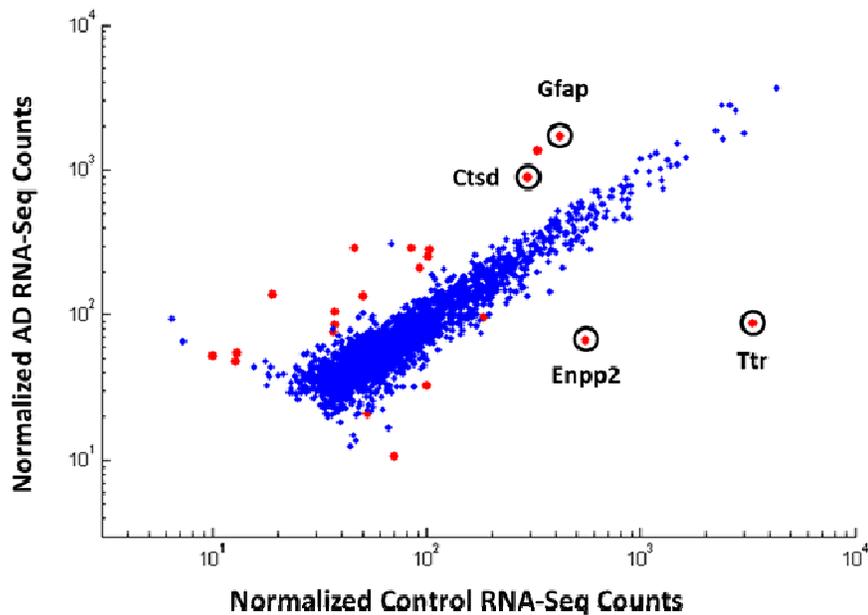addition to novel genes not previously linked to the disease (Supp. Table 3).

Figure 2. Differential gene expression in mouse hippocampus. Cuffdiff analysis of RNA-Sequencing

data found 2250 genes with altered expression in AD hippocampus. The top 24 most-changing genes (p

value from Cuffdiff ≤ 0.0005) are shown in red. Labeled genes were chosen for further detailed study based

on p value, fold change, and ontology.

Specific Genes Changing in the AD Hippocampus

Four significantly changing genes (Ttr, Gfap, Ctsd, and Enpp2) were chosen for

further analysis based on the initial evaluation of the list of differentially expressed

transcripts from Cuffdiff (Figure 3). Selection was based on significant differential

expression ($\geq 50\%$ increased or decreased expression), p value as determined by the

Cuffdiff software, and functional significance to AD. Differential expression of these genes was confirmed by qPCR (Supp. Figure 3).
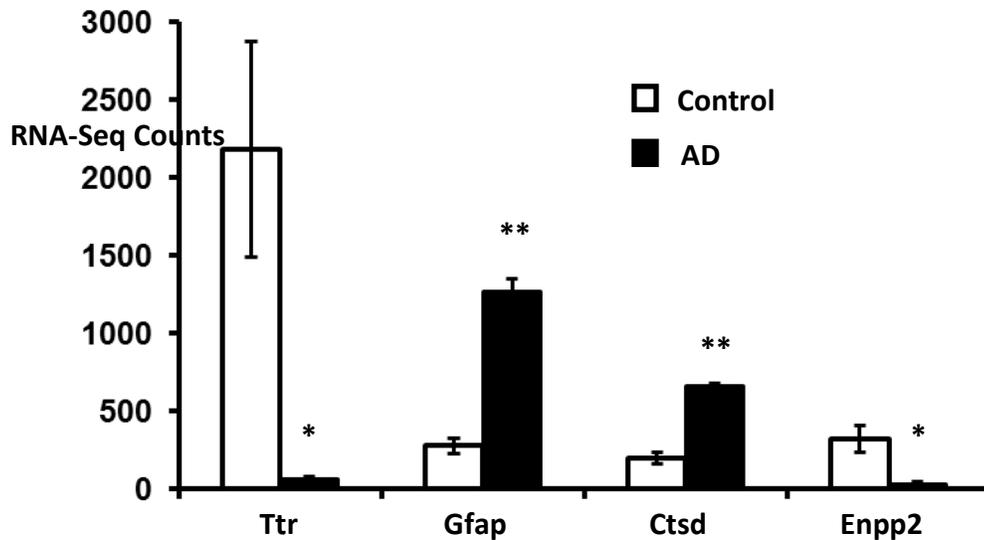

Figure 3. Differential expression of Ttr, Gfap, Ctsd, and Enpp2. Cufflinks and Cuffdiff analysis showed significant differential expression of Ttr, Gfap, Ctsd, and Enpp2 in AD mouse hippocampus. FPKM count data from Cufflinks are shown. * = pval <0.02 student's t-test; ** pval <0.001; error bars show SEM from three biological replicates. Enpp2 data corresponds to the Enpp2.1 variant transcript.

Differential Expression in Hippocampus vs. Differential Expression in Blood

Genome-wide expression data from hippocampus was compared to RNA-sequencing data from blood to identify possible biomarkers for AD diagnosis via a blood test (Figure 4). Blood data was also evaluated alone to develop a profile of changing gene expression in blood during AD development. Cuffdiff analysis showed 745 genes differentially expressed in AD blood, with 58 genes showing significant differential expression (p value calculated by Cuffdiff ≤ 0.05). The list of differentially expressed genes contained some genes linked to AD by previous studies as well as novel genes. Comparison of the 58 most-changing genes from blood with the 230 most-changing genes from hippocampus yielded 8 overlapping genes (Supp. Table 4). These genes could be targeted as potential biomarkers in the development of a blood test for AD diagnosis.
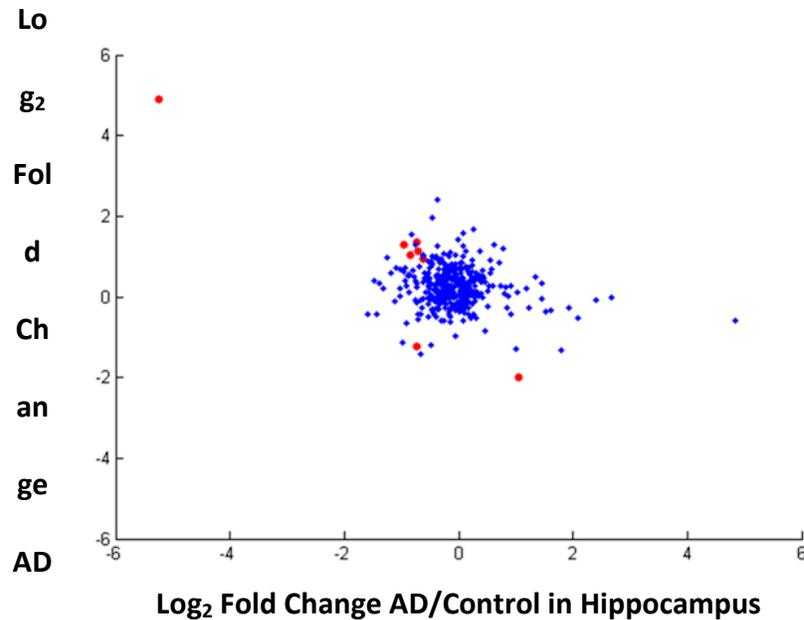
Figure 4. Correlation of hippocampal gene expression with blood gene expression. Comparison of RNA-sequencing data from blood to data from hippocampus showed potential biomarkers for a diagnostic AD blood test. Eight significantly changing genes (shown in red) were found to overlap in the blood and brain differential expression lists calculated by Cuffdiff.

Differential Expression of Genes vs. Isoforms in AD Hippocampus

RNA-sequencing data showed differential expression of genetic splice variants in AD hippocampus as well as of specific genes. Cuffdiff analysis gave two separate data sets: one containing expression data mapped to genes (with transcript variant data combined for each gene) and one containing expression data for individual transcripts. When transcript expression was evaluated, Cuffdiff showed 2205 splice variants differentially expressed in AD hippocampus. This included 205 transcripts with p value $\leq$ 0.05. When genes were assessed for differential expression without regard to splice variants, fewer differences were identified between control and AD samples than when isoform-specific differences were considered (Figure 5). This indicates a possible role for changing splice variant selection in disease development and the necessity of considering variant-specific differential expression in disease research.
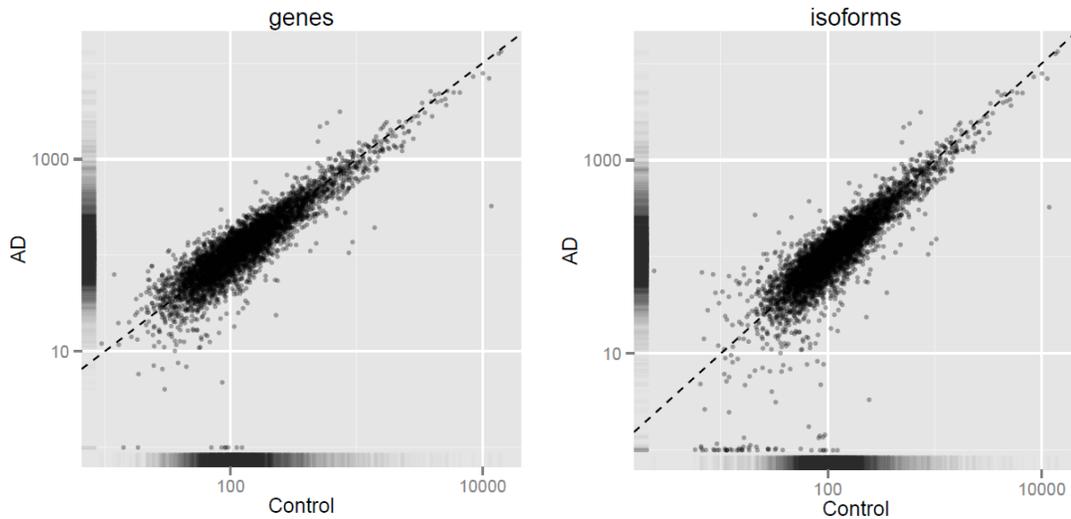
Figure 5. Differences between gene expression and isoform expression. RNA-sequencing revealed differential expression of both genes and gene isoforms in AD hippocampus. Normalized count data for AD and control samples are shown. Comparison of genome-wide expression for specific genes with expression of gene isoforms found that isoform/splice variant expression displays marked changes in the AD hippocampus, suggesting that splice variant selection could be relevant to AD pathology.

Discussion

Altered Expression of Mir 17

This study demonstrated significantly increased expression of microRNA 17 (Mir 17) in AD hippocampus, which could influence AD development by repression of various gene targets. MicroRNAs function in gene regulation by pairing to complementary mRNA targets. When this pairing occurs, the miRNA can either inhibit translation or lead to degradation of the mRNA [22]. MicroRNA control of gene expression has been shown to play a role in the development of many diseases including AD [22, 23]. A variety of microRNA genes have been shown to have altered expression in AD brain and blood [36, 37]. In addition, some microRNAs have specifically been implicated in APP processing [38].

The demonstrated change in expression of Mir 17 in an AD mouse model ($2^{0.731}$ or 1.66 fold change) agrees with previously determined data regarding the methylation status of this gene and indicates the importance of this microRNA in AD development. Methylation-specific chromatin immunoprecipitation and microarray analysis showed that the Mir 17 promoter region was significantly hypomethylated in the AD brain, suggesting that this gene might increase in expression in AD. The expected increase in expression was confirmed by differential expression analysis using qPCR. Previous research has shown that Mir 17 acts in regulation of the nervous system by reducing neuronal apoptosis. This occurs through Mir 17's repression of its target gene BMPRII (bone morphogenetic protein receptor II) [39]. Other studies have found that Mir 17 has multiple target genes involved in cell proliferation and has an overall effect of inducing neuronal cell proliferation through increased activity of E2F transcription factors [40]. When considered with the increased expression of Mir 17 shown by this study, this data suggests that Mir 17 upregulation caused by hypomethylation could function in the hippocampal response to neurodegeneration.

Decreased Expression of Ttr (Transthyretin)

The dramatic decrease in expression of Ttr (transthyretin) observed in AD hippocampus agreed with previous studies detailing the interaction between transthyretin and AD. Research indicates that the transthyretin protein can actually protect against amyloid plaques in AD [41]. Early studies found that transthyretin interacts with AB in CSF and inhibits formation of AB fibrils [42], and later researchers found that overexpression of transthyretin could restore cognitive function in some AD models [41, 42]. Other studies showed that transthyretin units join together to form a tetramer

structure which strongly binds AB oligomers. When transthyretin binds to AB in this way, the toxic AB aggregates characteristic of AD are unable to form [43]. Expression of Ttr would serve a protective role in AD by preventing the formation of AB plaques.

These studies explain the dramatic decrease in Ttr expression observed in the 5XFAD mouse model. RNA-Seq data showed that Ttr is strongly downregulated in AD hippocampus ($2^{-5.175}$ fold change). This would be expected given the inhibitory function of transthyretin with respect to AB. In order for AB deposits to form in these mice, transthyretin had to be decreased drastically—if functional transthyretin is present in any appreciable amount, AB cannot oligomerize to form senile plaques. Decreased expression of transthyretin allows AB plaques to develop and AD to progress, reinforcing the suggestions of previous researchers that Ttr could be an effective target in AD treatment. If normal expression of Ttr could be restored or supplemented, this might counteract the neurodegenerative accumulation of toxic AB oligomers that is a hallmark of AD pathology.

Increased Expression of Gfap (Glial Fibrillary Acidic Protein)

Increased expression of Gfap (glial fibrillary acidic protein) shown in an AD mouse model also extends the conclusions of previous studies. Gfap is an intermediate filament protein that serves a structural role in astrocytes, cells that serve a supportive role for neurons. In addition to its structural function, Gfap has also been implicated in neuronal regeneration, synaptic plasticity, and the response to neuronal damage [44]. This gene is known to be expressed in AD and has been associated with AB plaques. Although Gfap is normally expressed in astrocytes at some level, Gfap expression is known to increase when astrocytes switch from their normal quiescent state to a reactive state in

response to neuronal damage. Gfap expression usually increases in the localized areas surrounding AB plaques in AD. When Gfap expression is removed (as shown by experiments with Gfap knock-out mice), neurons become more sensitive to neurotoxicity and astrocytes become unable to surround AB plaques as they normally would [45].

Given the central role of Gfap in the astrocyte response to neuronal damage, increased expression of Gfap would be expected in the context of AD. Accumulation of AB deposits on the hippocampus leads to neurodegeneration, triggering the neuronal damage response by astrocytes. As astrocytes become reactive, Gfap should be upregulated to support the astrocytes' protective function of supporting damaged neurons and walling off AB plaques. RNA-Seq data from the hippocampus of our AD mouse model showed a significant increase in Gfap expression ($2^{2.084}$ fold change). This indicates that astrocytes in the hippocampus were responding to the damage caused by AB accumulation. The increase in Gfap expression shown in this model adds to current knowledge regarding the positive function of Gfap in the biological response to AB plaques.

Increased Expression of Ctsd (Cathepsin D)

The demonstrated increase in expression of Ctsd (cathepsin D) in the hippocampus of an AD mouse model is also interesting in light of previous research concerning the possible role of the cathepsin proteases in AD. Cathepsin D is an aspartic acid protease which has been suggested to play a role in the cleavage of APP to yield mature AB oligomers [46, 47]. Early investigation of cathepsin D indicated that it can act similarly to the beta-secretase enzymes thought to be the primary cause of APP cleavage to form AB [48]. This enzyme has been implicated in the processing pathways of both

AB and the tau proteins involved in neurofibrillary tangles, and some studies have

suggested that cathepsin D could be responsible for most beta-secretase activity in the

brain [46, 49]. In addition, cathepsin D levels have been shown to increase in AD

development [50].

The increased expression of Ctsd shown in this AD mouse model ($2^{1.632}$ fold

change) offers additional evidence that cathepsin D could play a role in APP cleavage to

yield AB plaques. If cathepsin D does function as a secretase enzyme to cleave APP and

form toxic AB oligomers, expression of Ctsd would be expected to increase with the

increased expression of APP resulting from the APP mutations in a transgenic mouse

model of AD. When combined with the activity of presenilin 1, increased activity of

cathepsin D would help accelerate the deposition of hippocampal AB plaques observed in

AD mice. This consideration has led some researchers to investigate the possible use of

cathepsin inhibitors as treatments for AD [50, 51].

Decreased Expression of Enpp2 (Autotaxin)

This study identified Enpp2 (ectonucleotide pyrophosphatase/phosphodiesterase 2

or autotaxin) as significantly changing in expression in the hippocampus of an AD mouse

model. Autotaxin acts to convert lysophosphatidylcholine to lysophosphatidic acid (LPA)

by lysophospholipase D activity. LPA can activate at least six G-protein coupled

receptors involved in a variety of cellular processes including cell proliferation, survival,

and migration [52]. This enzyme usually exists in a secreted form and can also function

in cell motility and growth [53]. No previous studies have found a connection between

autotaxin and AD development, but this protein has been linked to demyelination of

neurons through formation of LPA [54]. Other studies in zebrafish have found that

autotaxin plays a role in maturation of oligodendrocytes, which form the protective

myelin sheaths for neurons in the CNS [55].

The identification of Enpp2 as a significantly changing gene in AD highlights the

ability of genome-wide RNA-Seq studies like this one to discover previously unknown

factors affecting disease development. Enpp2/autotaxin remains a little-known protein,

and few studies have examined a connection between neuronal function and this enzyme.

However, genome-wide RNA-Seq data for this AD mouse model revealed significant

downregulation of Enpp2 ($2^{-3.042}$ fold change). Since autotaxin has been implicated in

oligodendrocyte function and cell survival, decreased expression of Enpp2 could

contribute to the neuronal loss seen in AD. Neurons already affected by deposition of AB

plaques could be further affected by loss of their protective myelin sheaths with

decreased expression of Enpp2. Further study detailing the function of autotaxin in AD

should be done to determine more specifically how this protein influences disease

development.

Gene vs. Isoform Differential Expression in the AD Hippocampus

The differences in expression of both genes and splice variants demonstrated by

RNA-sequencing are significant in the development of AD. Previous studies have shown

that genes related to stress response, inflammation, apoptotic pathways, angiogenesis, and

transcriptional regulation display altered expression in AD, and this study confirms those

changes [9]. Earlier research has also established time-sensitive effects of AB deposition

in the brain on gene expression [10, 11]. RNA-sequencing data from hippocampus in an

AD mouse model (known to develop AB plaques) reinforces the conclusions drawn by

those studies concerning the central importance of changing gene expression in AD.

Widespread changes in gene expression occur as AD develops in the brain, and these changes lead directly to the clinical effects of this disease.

In addition, changes in splice variant selection influence AD pathology. Many genes can be expressed as various different isoforms based on alternative splicing, and previous research has found that these alternative isoforms can be important in AD. For example, the Numb gene encodes four possible isoforms of a protein that interacts with APP. The specific isoform expressed helps to determine whether APP is degraded or recycled by the endosome pathway, influencing the development of AD [56]. This study demonstrated widespread changes in isoform expression as well as overall gene expression in AD, suggesting that splice variant switching may play an important role in disease development.

Blood Gene Expression as a Diagnostic Biomarker for AD

Comparison of RNA-sequencing data from blood with data from hippocampus revealed a set of 8 overlapping genes that show promise in the development of a diagnostic blood test for AD (Figure 6). Development of an efficient method for early AD diagnosis is a crucial area of disease research. Current medications for AD treatment are most effective if given early in disease progression, but most methods of AD diagnosis rely on behavioral signs not evident until later in disease development [4, 57, 58]. While PET scans, MRI, and tests of cerebrospinal fluid have been investigated as alternative diagnostic techniques, these methods are costly and sometimes invasive [10, 24, 58, 59]. These challenges have led many researchers to investigate the possibility of developing a blood test to diagnose AD [23, 60]. Since the hippocampus is known to be affected in characteristic ways by AB plaques and other characteristics of AD

development, parallel effects in the blood offer a target for diagnostic biomarkers of AD.

The 8 genes discovered by this study could be used to develop a blood gene expression

profile of AD, allowing diagnosis of the disease by a noninvasive and cost-effective
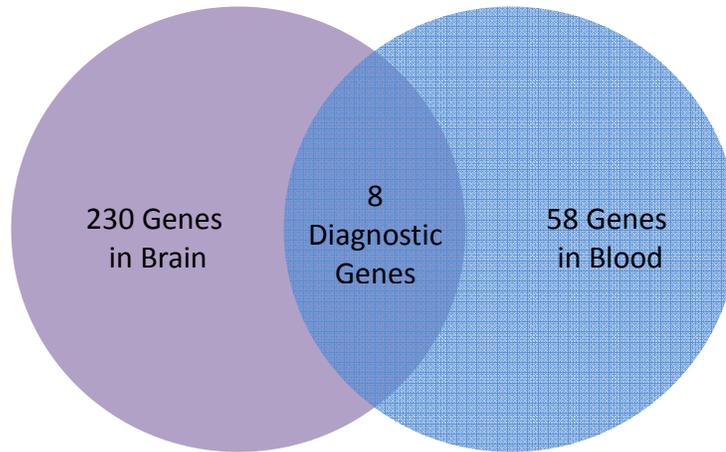
blood test.

Figure 6. Development of a blood gene expression profile for use in AD diagnosis. Comparison of gene

expression changes in hippocampus and blood for an AD mouse model revealed 8 overlapping genes that

could be used to develop a diagnostic profile for AD. The hippocampus is known to be strongly affected by

AD development with corresponding changes in cognitive function, and parallel changes in blood offer a

target for development of a noninvasive blood test to diagnose the disease.

AD Development and Diagnosis

Genome-wide RNA-sequencing analysis of differential gene expression in an AD

mouse model revealed significant changes in gene expression in both hippocampus and

blood. These changes directly affect AD pathology, and understanding these effects gives

better understanding of disease development as well as diagnosis and treatment options.

The overall changes in gene and splice variant expression shown by this study illustrate

the multiple interacting changes that result in AB plaques, NFTs, and clinical signs of

AD. The specific genes identified for study complement each other in a model for disease

development (Figure 7). As Ttr decreases expression in AD, neurons lose their protection

against AB, so plaques can freely form. Gfap increases in astrocyte development as the

neurons attempt to repair the damage caused by AB, while Ctsd increases formation of

AB plaques through secretase activity. Enpp2 contributes to regulation of the myelin

sheaths of neurons in the brain, while Mir 17 acts to support neuronal cell proliferation.

The other genes identified as differentially expressed in this study could play similar

roles by contributing to AD symptoms or aiding in the neuronal response to the disease.

These interacting changes result in the development of clinical AD. As researchers

continue to study these changes, this data will lead to better understanding of the disease

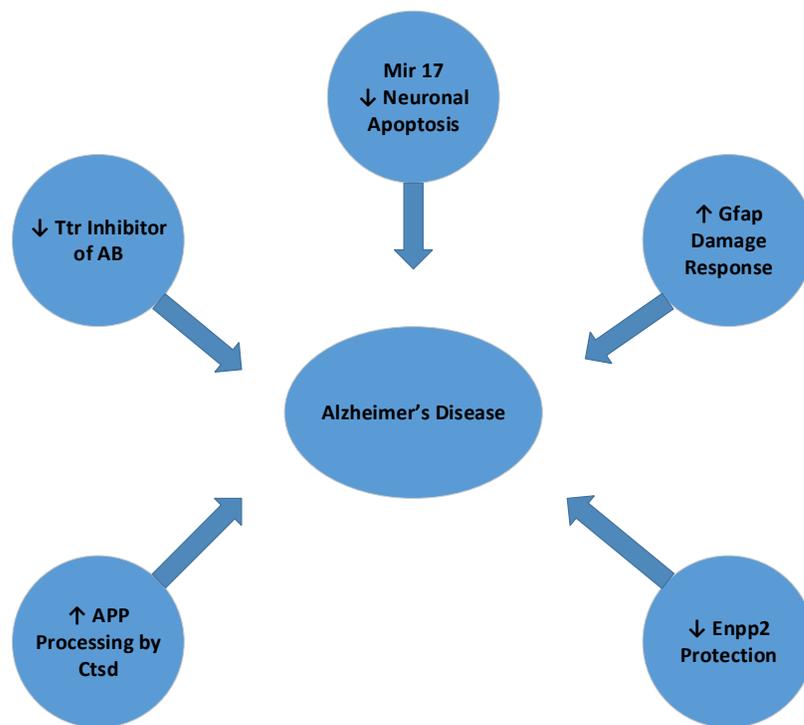and development of effective treatments.

Figure 7. Gene expression changes and AD. Interacting changes in gene expression contribute to the

development of Alzheimer's disease. In AD hippocampus, Ttr and Enpp2 lose their ability to protect

against neurodegeneration while Ctsd increases APP processing to form AB. Mir 17 and Gfap respond to

the disease by increasing expression to compensate for AB-induced damage.

Comparison of RNA-sequencing data from brain and blood gave a profile of eight changing genes that could be used to develop a diagnostic blood test for AD. Since the hippocampus exhibits distinctive changes in response to AD, altered gene expression in this region can be considered diagnostic of the disease. However, a practical and effective diagnostic requires biomarkers identifiable without histopathological examination of the hippocampus. Blood gene expression changes, which parallel changes in the hippocampus, could meet this requirement (Figure 8). Additional studies could be done to search for additional changing genes as well as to determine exactly when the expression profile observed here becomes evident in the blood. Future work should also investigate human brain and blood to confirm the validity of these results. If any or all of these eight genes are found to display altered expression early in AD development, they would be ideal for use as a diagnostic.
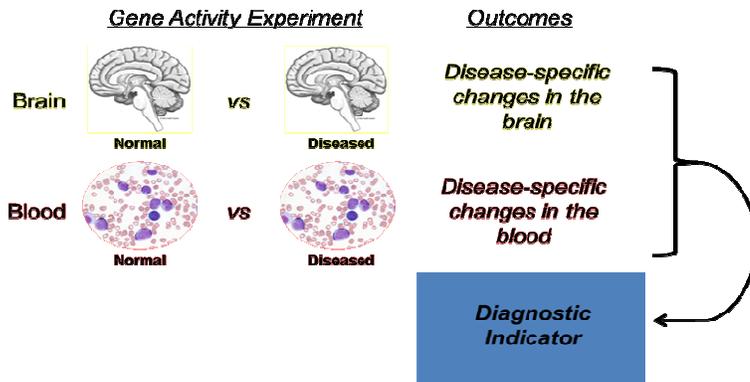

Figure 8. Gene expression and AD diagnosis. Comparison of AD-related changes in the brain to changes in the blood could be used to develop diagnostic biomarkers for AD. Specific gene expression changes in the brain are known to be linked to AD. If similar changes appear in the blood during disease development, these changes could be used to diagnose the disease via a blood test.

Conclusion

Alzheimer's disease changes millions of lives across the world, but modern medicine has yet to find a cure or even an easy method of diagnosis. For this reason, the two primary goals of this study were to find out exactly what happens in the brain as Alzheimer's disease develops and to discover an effective method of early disease diagnosis. Treatment for this disease requires an understanding of exactly what biological problems are causing it, and diagnosis requires identification of specific markers for AD. The analysis of changing genes in the AD brain performed in this study addressed the first of these goals by creating a picture of the overall changes underlying AD development. Hundreds of genes turn on and off to cause the loss of cognitive ability seen in AD, but certain genes stand out as possible targets for treatment. This study especially highlights the role of Ttr (transthyretin) in AD: if the gene for Ttr is "turned on," the protein deposits that characterize AD cannot form. Future research should investigate methods of restoring Ttr expression in AD to prevent or possibly reverse the effects of this disease. However, the most important result of this study is the panel of eight genes identified in both blood and brain as a possible diagnostic for AD. If these AD-specific changes could be developed into a diagnostic, AD could be diagnosed by a simple blood test even before symptoms occur. Medications could be given early in disease progression, when patients have the highest likelihood of successful treatment. To accomplish this goal, further research should test expression of these genes in blood at specific time points during AD development. When researchers confirm the ability of these genes to predict AD in mice, tests could be moved to clinical trials to predict disease in humans. Ideally, a predictive test for AD could be used for all patients at risk.

Through studies like this one, early detection and better treatment methods will be able to

help those affected by Alzheimer's disease.

Supplemental Figures
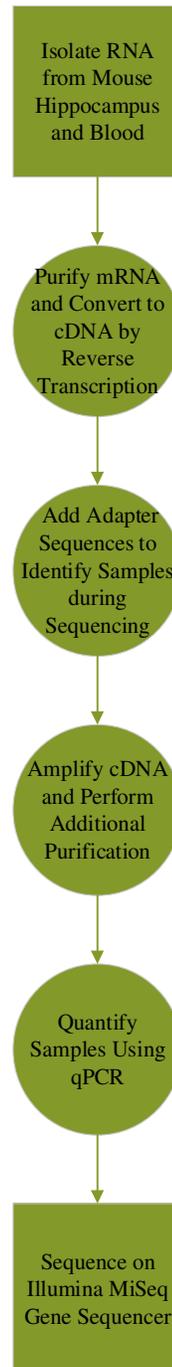
Supplemental Figure 1. Overview of RNA-sequencing process. Total RNA was isolated from

hippocampus and blood of three AD and three control mice. mRNA was purified using oligo-dT beads and

reverse transcribed to cDNA before additional purification. After adapter sequences were added to each

sample, cDNA was amplified and further purified before final quantification and sequencing.
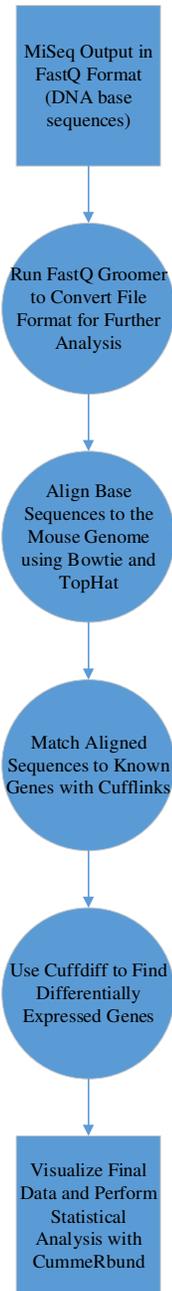
Supplemental Figure 2. Evaluation of differential gene expression using the Galaxy platform. Initial

sequencing output was formatted in FastQ files containing base sequences and quality data for the

sequencing run. The FastQ Groomer, FastQ Joiner, Bowtie, and TopHat programs were used to align

sequencing reads to the mouse genome before Cufflinks and Cuffdiff were used to identify differentially

expressed genes and transcripts. Further statistical analysis and graphing was performed using the

CummeRbund program.
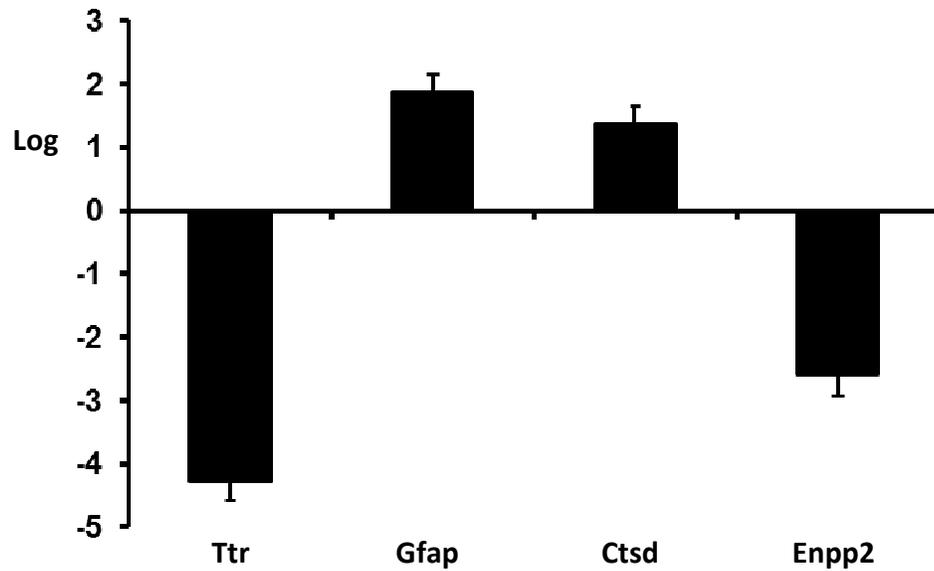
Supplemental Figure 3. Confirmation of top 4 differentially expressed genes. qPCR analysis confirmed significant differential expression of Ttr, Gfap, Ctsd, and Enpp2 in mouse hippocampus. Confirmations were performed for n=3 replicates using two different control genes (Gapdh and Tubb3). Error bars reflect SEM for n=6 (fold changes were calculated for three replicates with both control genes).

Supplemental Table 1. Genes decreasing expression in AD. Six genes were identified as having decreased expression in the AD hippocampus with p value ≤ 0.0005. These changing genes included some previously connected to AD as well as novel genes. "Known" indicates a well-defined function for this gene in AD pathology. "Associated" indicates that the gene has been linked to AD or neurobiology, but the specific function of the gene in the context of AD has not been extensively studied. "Novel" indicates no previous known connection to AD.

Symbol	Name	Log$_2$ Fold	P Value	AD Connection
Ttr	Transthyretin	-5.24	5.00E-05	Known [41-43]
Enpp2	Autotaxin	-3.02	5.00E-05	Novel [52-55]
Igf2	Insulin-like growth factor 2	-2.71	5.00E-05	Known [61-63]
Igfbp2	Insulin-like growth factor binding protein 2	-1.60	2.50E-04	Associated [11, 64, 65]
2900052N01Rik	RIKEN cDNA gene	-1.31	5.00E-05	Novel
Fam213a	Family with sequence similarity 213, member A	-0.93	4.50E-04	Novel

Supplemental Table 2. Genes increasing expression in AD. Sixteen genes were identified as having increased expression in the AD hippocampus with p value ≤ 0.0005. These changing genes included some with clear links to AD as well as lesser-known genes. "Known" indicates a well-defined function for this gene in AD pathology. "Associated" indicates that the gene has been linked to AD or neurobiology, but the specific function of the gene in the context of AD has not been extensively studied.

Symbol	Name	Log2 Fold	P Value	AD Connection
Igfbp5	Insulin-like growth factor binding protein 5	1.11	5.00E-05	Associated [66]
B2m	Beta-2 microglobulin	1.19	5.00E-04	Associated [67-70]
Hexa	Beta-hexosaminidase alpha subunit	1.23	2.50E-04	Associated [71, 72]
Ctss	Cathepsin S	1.35	5.00E-05	Known [73]
Ctsz	Cathepsin Z	1.46	3.00E-04	Known [73]
Hexb	Beta-hexosaminidase beta subunit	1.47	5.00E-05	Associated [71, 72]
Vim	Vimentin	1.52	5.00E-05	Known [74]
Ctsd	Cathepsin D	1.62	5.00E-05	Known [46-50]
C1qa	Complement component 1QA	1.79	5.00E-05	Known [75-78]
Laptm5	Lysosomal-associated protein transmembrane 5	1.93	3.50E-04	Known [79, 80]
Gfap	Glial fibrillary acidic protein	2.06	5.00E-05	Known [44, 45]
C4b	Complement component 4b	2.09	5.00E-05	Known [81]
Mpeg1	Macrophage expressed gene 1	2.41	5.00E-05	Known [77, 82]
Tyrobp	TYRO protein tyrosine kinase binding protein	2.68	1.50E-04	Known [83, 84]
Serpina3n	Serine peptidase inhibitor A3n	2.89	5.00E-05	Associated [85-87]
Cst7	Cystatin F	6.17	5.00E-05	Known [88, 89]

Supplemental Table 3. Ontological association of 22 most significant genes (p value ≤ 0.0005). Gene ontology (GO) analysis of the 22 most significant genes was performed using the GeneCodis program to group genes by biological process, cellular component, and molecular function [33-35]. Categories shown reflect biological functions or cellular locations most relevant to AD development.

Total Number of Genes	Gene Names	GO Category
6	Ctsz, Ctsd, Ctss, Hexb, Hexa, Laptm5	Located in lysosomes
6	Ctsz, Ctsd, Ctss, Hexb, Hexa, Enpp2	Hydrolase activity
5	Vim, Tyrobp, Gfap, Igf2, B2m	Protein binding
3	Ctsz, Ctsd, Ctss	Proteolysis
2	Vim, Gfap	Ganglioside catabolism Glial cell differentiation Astrocyte development
2	Hexb, Hexa	Lysosome organization Myelination Neuromuscular process controlling balance

Supplemental Table 4. Changing genes in both blood and brain. Eight genes showed significant differential expression in both hippocampus and blood for an AD mouse model. Overall data from Cuffdiff is shown for both data sets. *=0 value for Ttr in control blood was assigned a value of 1 for the purpose of fold calculations.

Symbol	Name	Log2 Fold Blood	P Value Blood	Log2 Fold Brain	P Value Brain
Ttr	Transthyretin	4.90*	5.00E-05	-5.24	5.00E-05
Scd1	Stearoyl-CoA desaturase 1	1.04	2.44E-02	-0.86	6.00E-04
C1qc	Complement component 1 subcomponent	-2.00	6.90E-03	1.06	4.50E-03
Pla2g7	Phospholipase A2, group 7	-1.21	1.86E-02	-0.74	4.55E-03
Syf2	Syf2 homolog, RNA splicing factor	1.30	2.11E-02	-0.96	4.70E-03
Sepp1	Selenoprotein P, plasma, 1	1.37	9.75E-03	-0.73	5.35E-03
Cox6a1	Cytochrome c oxidase subunit	0.93	4.51E-02	-0.62	2.21E-02
Hmgn1	High mobility group nucleosomal binding domain 1	1.14	3.40E-02	-0.70	3.09E-02

References

[1] Zawia NH, Lahiri DK, Cardozo-Pelaez F (2009) Epigenetics, oxidative stress, and Alzheimer disease. *Free Radic Biol Med* **46**, 1241-1249.

[2] Cacabelos R (2007) Molecular pathology and pharmacogenomics in Alzheimer's disease: polygenic-related effects of multifactorial treatments on cognition, anxiety and depression. *Methods Find Exp Clin Pharmacol* **29 Suppl A**, 1-91.

[3] Pohanka M (2013) Alzheimer s disease and oxidative stress: a review. *Curr Med Chem* **21**, 356-364.

[4] Samanta MK, Wilson B, Santhi K, Kumar KP, Suresh B (2006) Alzheimer disease and its management: a review. *Am J Ther* **13**, 516-526.

[5] Nelson PT, Alafuzoff I, Bigio EH, Bouras C, Braak H, Cairns NJ, Castellani RJ, Crain BJ, Davies P, Del Tredici K, Duyckaerts C, Frosch MP, Haroutunian V, Hof PR, Hulette CM, Hyman BT, Iwatsubo T, Jellinger KA, Jicha GA, Kovari E, Kukull WA, Leverenz JB, Love S, Mackenzie IR, Mann DM, Masliah E, McKee AC, Montine TJ, Morris JC, Schneider JA, Sonnen JA, Thal DR, Trojanowski JQ, Troncoso JC, Wisniewski T, Woltjer RL, Beach TG (2012) Correlation of Alzheimer disease neuropathologic changes with cognitive status: a review of the literature. *J Neuropathol Exp Neurol* **71**, 362-381.

[6] Coppieters N, Dragunow M (2011) Epigenetics in Alzheimer's disease: a focus on DNA modifications. *Curr Pharm Des* **17**, 3398-3412.

[7] Buxbaum JD, Christensen JL, Ruefli AA, Greengard P, Loring JF (1993) Expression of APP in brains of transgenic mice containing the entire human APP gene. *Biochem Biophys Res Commun* **197**, 639-645.

[8] Li Y, Zhou W, Tong Y, He G, Song W (2006) Control of APP processing and Abeta generation level by BACE1 enzymatic activity and transcription. *FASEB J* **20**, 285-292.

[9] Lukiw WJ (2004) Gene expression profiling in fetal, aged, and Alzheimer hippocampus: a continuum of stress-related signaling. *Neurochem Res* **29**, 1287-1297.

[10] Barucker C, Sommer A, Beckmann G, Eravci M, Harmeier A, Schipke CG, Brockschnieder D, Dyrks T, Althoff V, Fraser PE, Hazrati LN, George-Hyslop PS, Breitner JC, Peters O, Multhaup G (2014) Alzheimer Amyloid Peptide Abeta42 Regulates Gene Expression of Transcription and Growth Factors. *J Alzheimers Dis*.

[11] Rensink AA, Otte-Holler I, ten Donkelaar HJ, De Waal RM, Kremer B, Verbeek MM (2004) Differential gene expression in human brain pericytes induced by amyloid-beta protein. *Neuropathol Appl Neurobiol* **30**, 279-291.

[12]   Liu L, Li Y, Tollefsbol TO (2008) Gene-environment interactions and epigenetic basis of human diseases. *Curr Issues Mol Biol* **10**, 25-36.

[13]   Raiha I, Kaprio J, Koskenvuo M, Rajala T, Sourander L (1997) Alzheimer's disease in twins. *Biomed Pharmacother* **51**, 101-104.

[14]   Chen KL, Wang SS, Yang YY, Yuan RY, Chen RM, Hu CJ (2009) The epigenetic effects of amyloid-beta(1-40) on global DNA and neprilysin genes in murine cerebral endothelial cells. *Biochem Biophys Res Commun* **378**, 57-61.

[15]   Gatz M, Fratiglioni L, Johansson B, Berg S, Mortimer JA, Reynolds CA, Fiske A, Pedersen NL (2005) Complete ascertainment of dementia in the Swedish Twin Registry: the HARMONY study. *Neurobiol Aging* **26**, 439-447.

[16]   Gatz M, Pedersen NL, Berg S, Johansson B, Johansson K, Mortimer JA, Posner SF, Viitanen M, Winblad B, Ahlbom A (1997) Heritability for Alzheimer's disease: the study of dementia in Swedish twins. *J Gerontol A Biol Sci Med Sci* **52**, M117-125.

[17]   Irier HA, Jin P (2012) Dynamics of DNA methylation in aging and Alzheimer's disease. *DNA Cell Biol* **31 Suppl 1**, S42-48.

[18]   Mastroeni D, McKee A, Grover A, Rogers J, Coleman PD (2009) Epigenetic differences in cortical neurons from a pair of monozygotic twins discordant for Alzheimer's disease. *PLoS One* **4**, e6617.

[19]   Taher N, McKenzie C, Garrett R, Baker M, Fox N, Isaacs GD (2013) Amyloid-beta Alters the DNA Methylation Status of Cell-fate Genes in an Alzheimer's Disease Model. *J Alzheimers Dis*.

[20]   Sanchez-Mut JV, Aso E, Panayotis N, Lott I, Dierssen M, Rabano A, Urdinguio RG, Fernandez AF, Astudillo A, Martin-Subero JI, Balint B, Fraga MF, Gomez A, Gurnot C, Roux JC, Avila J, Hensch TK, Ferrer I, Esteller M (2013) DNA methylation map of mouse and human brain identifies target genes in Alzheimer's disease. *Brain* **136**, 3018-3027.

[21]   Cai Y, Yu X, Hu S, Yu J (2009) A brief review on the mechanisms of miRNA regulation. *Genomics Proteomics Bioinformatics* **7**, 147-154.

[22]   Slezak-Prochazka I, Durmus S, Kroesen BJ, van den Berg A (2010) MicroRNAs, macrocontrol: regulation of miRNA processing. *RNA* **16**, 1087-1095.

[23]   Leidinger P, Backes C, Deutscher S, Schmitt K, Mueller SC, Frese K, Haas J, Ruprecht K, Paul F, Stahler C, Lang CJ, Meder B, Bartfai T, Meese E, Keller A (2013) A blood based 12-miRNA signature of Alzheimer disease patients. *Genome Biol* **14**, R78.

[24]   Jellinger KA, Janetzky B, Attems J, Kienzl E (2008) Biomarkers for early diagnosis of Alzheimer disease: 'ALZheimer ASsociated gene'--a new blood biomarker? *J Cell Mol Med* **12**, 1094-1117.

[25]   Bai Z, Stamova B, Xu H, Ander BP, Wang J, Jickling GC, Zhan X, Liu D, Han G, Jin LW, DeCarli C, Lei H, Sharp FR (2014) Distinctive RNA expression profiles in blood associated with Alzheimer disease after accounting for white matter hyperintensities. *Alzheimer Dis Assoc Disord* **28**, 226-233.

[26]   Oakley H, Cole SL, Logan S, Maus E, Shao P, Craft J, Guillozet-Bongaarts A, Ohno M, Disterhoft J, Van Eldik L, Berry R, Vassar R (2006) Intraneuronal beta-amyloid aggregates, neurodegeneration, and neuron loss in transgenic mice with five familial Alzheimer's disease mutations: potential factors in amyloid plaque formation. *J Neurosci* **26**, 10129-10140.

[27]   Bartoo GT, Nochlin D, Chang D, Kim Y, Sumi SM (1997) The mean A beta load in the hippocampus correlates with duration and severity of dementia in subgroups of Alzheimer disease. *J Neuropathol Exp Neurol* **56**, 531-540.

[28]   Maldjian JA, Whitlow CT (2012) Whither the hippocampus? FDG-PET hippocampal hypometabolism in Alzheimer disease revisited. *AJNR Am J Neuroradiol* **33**, 1975-1982.

[29]   Blankenberg D, Gordon A, Von Kuster G, Coraor N, Taylor J, Nekrutenko A (2010) Manipulation of FASTQ data with Galaxy. *Bioinformatics* **26**, 1783-1785.

[30]   Trapnell C, Pachter L, Salzberg SL (2009) TopHat: discovering splice junctions with RNA-Seq. *Bioinformatics* **25**, 1105-1111.

[31]   Trapnell C, Williams BA, Pertea G, Mortazavi A, Kwan G, van Baren MJ, Salzberg SL, Wold BJ, Pachter L (2010) Transcript assembly and quantification by RNA-Seq reveals unannotated transcripts and isoform switching during cell differentiation. *Nat Biotechnol* **28**, 511-515.

[32]   Trapnell C, Roberts A, Goff L, Pertea G, Kim D, Kelley DR, Pimentel H, Salzberg SL, Rinn JL, Pachter L (2012) Differential gene and transcript expression analysis of RNA-seq experiments with TopHat and Cufflinks. *Nat Protoc* **7**, 562-578.

[33]   Tabas-Madrid D, Nogales-Cadenas R, Pascual-Montano A (2012) GeneCodis3: a non-redundant and modular enrichment analysis tool for functional genomics. *Nucleic Acids Res* **40**, W478-483.

[34]   Nogales-Cadenas R, Carmona-Saez P, Vazquez M, Vicente C, Yang X, Tirado F, Carazo JM, Pascual-Montano A (2009) GeneCodis: interpreting gene lists through enrichment analysis and integration of diverse biological information. *Nucleic Acids Res* **37**, W317-322.

[35]   Carmona-Saez P, Chagoyen M, Tirado F, Carazo JM, Pascual-Montano A (2007) GENECODIS: a web-based tool for finding significant concurrent annotations in gene lists. *Genome Biol* **8**, R3.

[36]   Shioya M, Obayashi S, Tabunoki H, Arima K, Saito Y, Ishida T, Satoh J (2010) Aberrant microRNA expression in the brains of neurodegenerative diseases: miR-29a decreased in Alzheimer disease brains targets neurone navigator 3. *Neuropathol Appl Neurobiol* **36**, 320-330.

[37]   Villa C, Ridolfi E, Fenoglio C, Ghezzi L, Vimercati R, Clerici F, Marcone A, Gallone S, Serpente M, Cantoni C, Bonsi R, Cioffi S, Cappa S, Franceschi M, Rainero I, Mariani C, Scarpini E, Galimberti D (2013) Expression of the transcription factor Sp1 and its regulatory hsa-miR-29b in peripheral blood mononuclear cells from patients with Alzheimer's disease. *J Alzheimers Dis* **35**, 487-494.

[38]   Wang WX, Rajeev BW, Stromberg AJ, Ren N, Tang G, Huang Q, Rigoutsos I, Nelson PT (2008) The expression of microRNA miR-107 decreases early in Alzheimer's disease and may accelerate disease progression through regulation of beta-site amyloid precursor protein-cleaving enzyme 1. *J Neurosci* **28**, 1213-1223.

[39]   Sun Q, Mao S, Li H, Zen K, Zhang CY, Li L (2013) Role of miR-17 family in the negative feedback loop of bone morphogenetic protein signaling in neuron. *PLoS One* **8**, e83067.

[40]   Trompeter HI, Abbad H, Iwaniuk KM, Hafner M, Renwick N, Tuschl T, Schira J, Muller HW, Wernet P (2011) MicroRNAs MiR-17, MiR-20a, and MiR-106b act in concert to modulate E2F activity on cell cycle arrest during neuronal lineage differentiation of USSC. *PLoS One* **6**, e16138.

[41]   Buxbaum JN, Reixach N (2009) Transthyretin: the servant of many masters. *Cell Mol Life Sci* **66**, 3095-3101.

[42]   Li X, Buxbaum JN (2011) Transthyretin and the brain re-visited: is neuronal synthesis of transthyretin protective in Alzheimer's disease? *Mol Neurodegener* **6**, 79.

[43]   Yang DT, Joshi G, Cho PY, Johnson JA, Murphy RM (2013) Transthyretin as both a sensor and a scavenger of beta-amyloid oligomers. *Biochemistry* **52**, 2849-2861.

[44]   Middeldorp J, Hol EM (2011) GFAP in health and disease. *Prog Neurobiol* **93**, 421-443.

[45]   Kamphuis W, Mamber C, Moeton M, Kooijman L, Sluijs JA, Jansen AH, Verveer M, de Groot LR, Smith VD, Rangarajan S, Rodriguez JJ, Orre M, Hol EM (2012) GFAP isoforms in adult mouse brain with a focus on neurogenic astrocytes and reactive astrogliosis in mouse models of Alzheimer disease. *PLoS One* **7**, e42823.

[46]   Mariani E, Seripa D, Ingegni T, Nocentini G, Mangialasche F, Ercolani S, Cherubini A, Metastasio A, Pilotto A, Senin U, Mecocci P (2006) Interaction of CTSD and A2M polymorphisms in the risk for Alzheimer's disease. *J Neurol Sci* **247**, 187-191.

[47]   Sadik G, Kaji H, Takeda K, Yamagata F, Kameoka Y, Hashimoto K, Miyanaga K, Shinoda T (1999) In vitro processing of amyloid precursor protein by cathepsin D. *Int J Biochem Cell Biol* **31**, 1327-1337.

[48]   Chevallier N, Vizzavona J, Marambaud P, Baur CP, Spillantini M, Fulcrand P, Martinez J, Goedert M, Vincent JP, Checler F (1997) Cathepsin D displays in vitro beta-secretase-like specificity. *Brain Res* **750**, 11-19.

[49]   Schechter I, Ziv E (2008) Kinetic properties of cathepsin D and BACE 1 indicate the need to search for additional beta-secretase candidate(s). *Biol Chem* **389**, 313-320.

[50]   Haque A, Banik NL, Ray SK (2008) New insights into the roles of endolysosomal cathepsins in the pathogenesis of Alzheimer's disease: cathepsin inhibitors as potential therapeutics. *CNS Neurol Disord Drug Targets* **7**, 270-277.

[51]   Hook V, Toneff T, Bogyo M, Greenbaum D, Medzihradszky KF, Neveu J, Lane W, Hook G, Reisine T (2005) Inhibition of cathepsin B reduces beta-amyloid production in regulated secretory vesicles of neuronal chromaffin cells: evidence for cathepsin B as a candidate beta-secretase of Alzheimer's disease. *Biol Chem* **386**, 931-940.

[52]   Saga H, Ohhata A, Hayashi A, Katoh M, Maeda T, Mizuno H, Takada Y, Komichi Y, Ota H, Matsumura N, Shibaya M, Sugiyama T, Nakade S, Kishikawa K (2014) A novel highly potent autotaxin/ENPP2 inhibitor produces prolonged decreases in plasma lysophosphatidic acid formation in vivo and regulates urethral tension. *PLoS One* **9**, e93230.

[53]   Koike S, Keino-Masu K, Ohto T, Masu M (2006) The N-terminal hydrophobic sequence of autotaxin (ENPP2) functions as a signal peptide. *Genes Cells* **11**, 133-142.

[54]   Nagai J, Uchida H, Matsushita Y, Yano R, Ueda M, Niwa M, Aoki J, Chun J, Ueda H (2010) Autotaxin and lysophosphatidic acid1 receptor-mediated demyelination of dorsal root fibers by sciatic nerve injury and intrathecal lysophosphatidylcholine. *Mol Pain* **6**, 78.

[55]   Yuelling LW, Waggener CT, Afshari FS, Lister JA, Fuss B (2012) Autotaxin/ENPP2 regulates oligodendrocyte differentiation in vivo in the developing zebrafish hindbrain. *Glia* **60**, 1605-1618.

[56]   Kyriazis GA, Wei Z, Vandermey M, Jo DG, Xin O, Mattson MP, Chan SL (2008) Numb endocytic adapter proteins regulate the transport and processing of the

amyloid precursor protein in an isoform-dependent manner: implications for Alzheimer disease pathogenesis. *J Biol Chem* **283**, 25492-25502.

[57]   Barker WW, Luis C, Harwood D, Loewenstein D, Bravo M, Ownby R, Duara R (2005) The effect of a memory screening program on the early diagnosis of Alzheimer disease. *Alzheimer Dis Assoc Disord* **19**, 1-7.

[58]   Jelic V, Nordberg A (2000) Early diagnosis of Alzheimer disease with positron emission tomography. *Alzheimer Dis Assoc Disord* **14 Suppl 1**, S109-113.

[59]   McMahon PM, Araki SS, Neumann PJ, Harris GJ, Gazelle GS (2000) Cost-effectiveness of functional imaging tests in the diagnosis of Alzheimer disease. *Radiology* **217**, 58-68.

[60]   Lunnon K, Sattlecker M, Furney SJ, Coppola G, Simmons A, Proitsi P, Lupton MK, Lourdusamy A, Johnston C, Soininen H, Kloszewska I, Mecocci P, Tsolaki M, Vellas B, Geschwind D, Lovestone S, Dobson R, Hodges A (2013) A blood gene expression marker of early Alzheimer's disease. *J Alzheimers Dis* **33**, 737-753.

[61]   Bracko O, Singer T, Aigner S, Knobloch M, Winner B, Ray J, Clemenson GD, Jr., Suh H, Couillard-Despres S, Aigner L, Gage FH, Jessberger S (2012) Gene expression profiling of neural stem cells and their neuronal progeny reveals IGF2 as a regulator of adult hippocampal neurogenesis. *J Neurosci* **32**, 3376-3387.

[62]   Harper KM, Tunc-Ozcan E, Graf EN, Herzing LB, Redei EE (2014) Intergenerational and parent of origin effects of maternal calorie restriction on Igf2 expression in the adult rat hippocampus. *Psychoneuroendocrinology* **45**, 187-191.

[63]   Mellott TJ, Pender SM, Burke RM, Langley EA, Blusztajn JK (2014) IGF2 ameliorates amyloidosis, increases cholinergic marker expression and raises BMP9 and neurotrophin levels in the hippocampus of the APPswePS1dE9 Alzheimer's disease model mice. *PLoS One* **9**, e94287.

[64]   Pedros I, Petrov D, Allgaier M, Sureda F, Barroso E, Beas-Zarate C, Auladell C, Pallas M, Vazquez-Carrera M, Casadesus G, Folch J, Camins A (2014) Early alterations in energy metabolism in the hippocampus of APPswe/PS1dE9 mouse model of Alzheimer's disease. *Biochim Biophys Acta* **1842**, 1556-1566.

[65]   Toledo JB, Da X, Bhatt P, Wolk DA, Arnold SE, Shaw LM, Trojanowski JQ, Davatzikos C (2013) Relationship between plasma analytes and SPARE-AD defined brain atrophy patterns in ADNI. *PLoS One* **8**, e55531.

[66]   Barucker C, Sommer A, Beckmann G, Eravci M, Harmeier A, Schipke CG, Brockschnieder D, Dyrks T, Althoff V, Fraser PE, Hazrati LN, George-Hyslop PS, Breitner JC, Peters O, Multhaup G (2015) Alzheimer amyloid Peptide abeta42

regulates gene expression of transcription and growth factors. *J Alzheimers Dis* **44**, 613-624.

[67]   Bellotti V, Mangione P, Stoppini M (1999) Biological activity and pathological implications of misfolded proteins. *Cell Mol Life Sci* **55**, 977-991.

[68]   Carrette O, Demalte I, Scherl A, Yalkinoglu O, Corthals G, Burkhard P, Hochstrasser DF, Sanchez JC (2003) A panel of cerebrospinal fluid potential biomarkers for the diagnosis of Alzheimer's disease. *Proteomics* **3**, 1486-1494.

[69]   Davidsson P, Westman-Brinkmalm A, Nilsson CL, Lindbjer M, Paulson L, Andreasen N, Sjogren M, Blennow K (2002) Proteome analysis of cerebrospinal fluid proteins in Alzheimer patients. *Neuroreport* **13**, 611-615.

[70]   Doecke JD, Laws SM, Faux NG, Wilson W, Burnham SC, Lam CP, Mondal A, Bedo J, Bush AI, Brown B, De Ruyck K, Ellis KA, Fowler C, Gupta VB, Head R, Macaulay SL, Pertile K, Rowe CC, Rembach A, Rodrigues M, Rumble R, Szoeke C, Taddei K, Taddei T, Trounson B, Ames D, Masters CL, Martins RN (2012) Blood-based protein biomarkers for diagnosis of Alzheimer disease. *Arch Neurol* **69**, 1318-1325.

[71]   Magini A, Polchi A, Tozzi A, Tancini B, Tantucci M, Urbanelli L, Borsello T, Calabresi P, Emiliani C (2015) Abnormal cortical lysosomal beta-hexosaminidase and beta-galactosidase activity at post-synaptic sites during Alzheimer's disease progression. *Int J Biochem Cell Biol* **58**, 62-70.

[72]   Tiribuzi R, Orlacchio A, Crispoltoni L, Maiotti M, Zampolini M, De Angeliz M, Mecocci P, Cecchetti R, Bernardi G, Datti A, Martino S (2011) Lysosomal beta-galactosidase and beta-hexosaminidase activities correlate with clinical stages of dementia associated with Alzheimer's disease and type 2 diabetes mellitus. *J Alzheimers Dis* **24**, 785-797.

[73]   Bernstein HG, Kirschke H, Wiederanders B, Pollak KH, Zipress A, Rinne A (1996) The possible place of cathepsins and cystatins in the puzzle of Alzheimer disease: a review. *Mol Chem Neuropathol* **27**, 225-247.

[74]   Levin EC, Acharya NK, Sedeyn JC, Venkataraman V, D'Andrea MR, Wang HY, Nagele RG (2009) Neuronal expression of vimentin in the Alzheimer's disease brain may be part of a generalized dendritic damage-response mechanism. *Brain Res* **1298**, 194-207.

[75]   Benoit ME, Hernandez MX, Dinh ML, Benavente F, Vasquez O, Tenner AJ (2013) C1q-induced LRP1B and GPR6 proteins expressed early in Alzheimer disease mouse models, are essential for the C1q-mediated protection against amyloid-beta neurotoxicity. *J Biol Chem* **288**, 654-665.

[76]   Crehan H, Hardy J, Pocock J (2012) Microglia, Alzheimer's disease, and complement. *Int J Alzheimers Dis* **2012**, 983640.

[77] Eikelenboom P, Veerhuis R (1996) The role of complement and activated microglia in the pathogenesis of Alzheimer's disease. *Neurobiol Aging* **17**, 673-680.

[78] Rogers J, Webster S, Lue LF, Brachova L, Civin WH, Emmerling M, Shivers B, Walker D, McGeer P (1996) Inflammation and Alzheimer's disease pathogenesis. *Neurobiol Aging* **17**, 681-686.

[79] Zheng L, Roberg K, Jerhammar F, Marcusson J, Terman A (2006) Oxidative stress induces intralysosomal accumulation of Alzheimer amyloid beta-protein in cultured neuroblastoma cells. *Ann N Y Acad Sci* **1067**, 248-251.

[80] Maxfield FR (2014) Role of endosomes and lysosomes in human disease. *Cold Spring Harb Perspect Biol* **6**, a016931.

[81] Trouw LA, Nielsen HM, Minthon L, Londos E, Landberg G, Veerhuis R, Janciauskiene S, Blom AM (2008) C4b-binding protein in Alzheimer's disease: binding to Abeta1-42 and to dead cells. *Mol Immunol* **45**, 3649-3660.

[82] Wada R, Tifft CJ, Proia RL (2000) Microglial activation precedes acute neurodegeneration in Sandhoff disease and is suppressed by bone marrow transplantation. *Proc Natl Acad Sci U S A* **97**, 10954-10959.

[83] Wunderlich P, Glebov K, Kemmerling N, Tien NT, Neumann H, Walter J (2013) Sequential proteolytic processing of the triggering receptor expressed on myeloid cells-2 (TREM2) protein by ectodomain shedding and gamma-secretase-dependent intramembranous cleavage. *J Biol Chem* **288**, 33027-33036.

[84] Zhang B, Gaiteri C, Bodea LG, Wang Z, McElwee J, Podtelezhnikov AA, Zhang C, Xie T, Tran L, Dobrin R, Fluder E, Clurman B, Melquist S, Narayanan M, Suver C, Shah H, Mahajan M, Gillis T, Mysore J, MacDonald ME, Lamb JR, Bennett DA, Molony C, Stone DJ, Gudnason V, Myers AJ, Schadt EE, Neumann H, Zhu J, Emilsson V (2013) Integrated systems approach identifies genetic nodes and networks in late-onset Alzheimer's disease. *Cell* **153**, 707-720.

[85] Lucotte B, Tajhizi M, Alkhatib D, Samuelsson EB, Wiehager B, Schedin-Weiss S, Sundstrom E, Winblad B, Tjernberg LO, Behbahani H (2014) Stress Conditions Increase Vimentin Cleavage by Omi/HtrA2 Protease in Human Primary Neurons and Differentiated Neuroblastoma Cells. *Mol Neurobiol*.

[86] Swiderski RE, Nishimura DY, Mullins RF, Olvera MA, Ross JL, Huang J, Stone EM, Sheffield VC (2007) Gene expression analysis of photoreceptor cell loss in bbs4-knockout mice reveals an early stress gene response and photoreceptor cell damage. *Invest Ophthalmol Vis Sci* **48**, 3329-3340.

[87] Switonski PM, Szlachcic WJ, Krzyzosiak WJ, Figiel M (2015) A new humanized ataxin-3 knock-in mouse model combines the genetic features, pathogenesis of

neurons and glia and late disease onset of SCA3/MJD. *Neurobiol Dis* **73**, 174-188.

[88]   Yang DS, Stavrides P, Saito M, Kumar A, Rodriguez-Navarro JA, Pawlik M, Huo C, Walkley SU, Cuervo AM, Nixon RA (2014) Defective macroautophagic turnover of brain lipids in the TgCRND8 Alzheimer mouse model: prevention by correcting lysosomal proteolytic deficits. *Brain* **137**, 3300-3318.

[89]   Small DH, Hu Y, Bolos M, Dawkins E, Foa L, Young KM (2014) beta-Amyloid precursor protein: function in stem cell development and Alzheimer's disease brain. *Neurodegener Dis* **13**, 96-98.